*Kidney International, Vol. 67 (2005), pp. 576–591*

# Crystal-associated nephropathy in patients with brushite nephrolithiasis

**ANDREW P. EVAN, JAMES E. LINGEMAN, FREDRIC L. COE, YOUZHI SHAO, JOAN H. PARKS, SHARON B. BLEDSOE, CARRIE L. PHILLIPS, STEPHEN BONSIB, ELAINE M. WORCESTER, ANDRE J. SOMMER, SAM C. KIM, WILLIAM W. TINMOUTH, and MARC GRYNPAS**

*Department of Anatomy and Cell Biology, Indiana University School of Medicine, Indianapolis, Indiana; Methodist Hospital Institute for Kidney Stone Disease, Indianapolis, Indiana; Nephrology Section, University of Chicago, Chicago, Illinois; Department of Histology, Jinzhou Medical College, Jinzhou, Liaoning, Peoples Republic of China; Department of Pathology, Indiana University School of Medicine, Indianapolis, Indiana; Department of Chemistry and Biochemistry, Miami University, Oxford, Ohio; and Samuel Lunenfeld Research Institute, Mount Sinai Hospital, Toronto, Canada*

**Crystal-associated nephropathy in patients with brushite nephrolithiasis.**

*Background.* We have biopsied the renal cortex and papillae of patients who form brushite renal stones asking if this unusual stone type is associated with specific tissue changes. We contrasted these with biopsies of 15 calcium oxalate stone formers, three stone formers with intestinal bypass, and four normal subjects.

*Methods.* We studied all ten brushite stone formers treated with percutaneous nephrolithotomy (PNL) during the past 3 years using digital video imaging of renal papillae, and obtained cortical and papillary biopsies. Biopsies were analyzed by light and electron microscopy, microinfrared spectroscopy, and electron diffraction.

*Results.* Apatite crystals plugged scattered terminal collecting ducts whose cells were injured or dead, and surrounding interstitium inflamed and fibrotic. White papillary deposits of interstitial apatite particles, so called Randall's plaque, were also present. Glomerular changes and cortical tubular atrophy and interstitial fibrosis were moderate to severe.

*Conclusion.* Brushite stone formers combine the interstitial plaque of calcium oxalate stone formers with the collecting duct apatite plugs found in stone formers with intestinal bypass. Collecting duct injury and interstitial fibrosis are severe. Prominent cortical fibrosis, tubule atrophy, and glomerular pathology seem secondary to the collecting duct plugging. We believe crystallization obstructs and destroys terminal collecting duct segments thereby damaging nephrons, perhaps via intranephronal obstruction, and producing a hitherto unrecognized renal disease.

**Key words:** kidney calculi, calcium phosphate, extracorporeal shockwave lithotripsy.

Received for publication July 2, 2004
and in revised form August 3, 2004, and August 23, 2004
Accepted for publication September 1, 2004



About 5% of people form renal stones usually made of calcium oxalate [1]. In biopsy samples taken during percutaneous nephrolithotomy (PNL) we have found that the common calcium oxalate stone formers produce interstitial apatite particles that form the well-known Randall's plaques [2], but do not damage epithelial cells or cause interstitial inflammation or fibrosis. Among stone formers with intestinal bypass for obesity we found no plaque, but some terminal collecting duct lumens were plugged with apatite crystals associated with epithelial cell damage and inflammation and fibrosis of the surrounding interstitium. In other words, the two kinds of stone formers displayed specific pathologies.

About 15% of stone formers produce predominantly (>50%) calcium phosphate stones; of these, one fourth form stones containing brushite ($CaHPO_4$) [3]. We report here renal papillary morphology and histopathology of all ten brushite stone formers we have treated with PNL during the past 3 years. Like calcium oxlate stone formers, brushite stone formers have interstitial plaque. Like bypass stone formers, they have apatite crystallization within terminal collecting duct, associated with collecting duct cell death, and papillary interstitial inflammation and fibrosis. In other words, their pathology is an amalgam of calcium oxalate and bypass stone disease; but collecting duct plugging and cell injury are far more severe, as is interstitial inflammation and fibrosis.

The severity of the collecting duct and papillary interstitial disease led us to evaluate cortical injury in the brushite stone formers and compare it to our prior calcium oxalate and bypass stone formers and nonstone forming controls, asking if the more severe papillary injury among brushite stone formers leads to proportionately more severe glomerular changes, tubule atrophy, and interstitial fibrosis. The papillary and cortical abnormalities in brushite stone formers are in fact so marked

**Table 1.** Clinical characteristics of biopsied patients

| Case | Gender | Age first stone | Number of stones | ESWL | PNL | Number of procedures | Age at Bx | %brushite | Relatives |
|---|---|---|---|---|---|---|---|---|---|
| 1 | F | 42 | 2 | 1 (1) | 1 (1) | 2 (2) | 42 | 100 (100) | 6 (1) |
| 2[a] | F | 14 | 25 | 11 (5) | 1 (1) | 13 (6) | 42 | 70 (100) | 13 (1) |
| 3 | F | 18 | >30 | 11 (8) | 1 (1) | 29 (18) | 59 | 0 (100) | 16 (5) |
| 4[b] | M | 7 | 23 | 10 (9) | 1 (1) | 16 (13) | 23 | 98 (100) | 3 (1) |
| 5 | M | 31 | 30 | 3 (2) | 2 (1) | 11 (6) | 42 | 0 (65) | n/a |
| 6 | M | 17 | >30 | 5 (3) | 2 (2) | 14 (10) | 64 | 98 (100) | 13 (8) |
| 7[c] | M | 45 | 10 | 0 | 1 (1) | 7 (7) | 52 | 0 (100) | 3 (2) |
| 8 | M | 18 | 18 | 6 (4) | 5 (2) | 23 (11) | 31 | 0 (100) | 3 (1) |
| 9 | F | 22 | 10 | 5 (2) | 0 | 9 (6) | 44 | 0 (100) | 7 (1) |
| 10[d] | M | 28 | 9 | 1 (1) | 4 (3) | 10 (8) | 39 | 100 (100) | 1 (1) |

Abbreviations: Br, . . . ; stones, number of stones before Bx; ESWL, extracorporeal shock wave lithotripsy before bx (Bx side); PNL, percutaneous nephrolithotomy before Bx (Bx side); procedures, total of all procedures (includes ESWL, PNL, ureteroscopy, open surgery, cystolithopaxy) before Bx (Bx side); %brushite, percent brushite in first available analysis (% in most recent analysis); relatives, number of first degree relatives (number with stones).

[a] Case 2 had high blood pressure, multiple urinary tract infections.

[b] Case 4 had dismembered pyeloplasty age 4 for ureteropelvic junction obstruction, first stone soon after.

[c] Case 7 was chronic uric acid stone former and received extensive potassium citrate treatment for stone dissolution and formed a brushite stone.

[d] Case 10 was rendered c4/5 quadriplegic at age 22; multiple pseudomonas urinary tract infections treated mainly with aminoglycosides.

as to constitute a significant and hitherto unrecognized renal disease not present in calcium oxalate or bypass stone formers. Although mechanisms are not as yet entirely clear, crystal formation seems a reasonable initiating cause, with consequent collecting duct cell injury, eventual destruction of terminal collecting duct segments, and resulting nephron damage and loss.

## METHODS

### Subjects

We studied ten brushite stone formers, who represent all calcium phosphate stone formers requiring PNL at our institution in a 3-year period. Clinical history was obtained, along with reviews of old records to obtain stone analyses and type and number of stone procedures (Table 1). In every case, the most recent stone contained 65% or more brushite. In addition, we analyzed renal cortical pathology of 15 calcium oxalate stone formers, three patients with calcium oxalate stones after intestinal bypass for obesity, and four nonstone forming patients, who had undergone nephrectomy for other reasons. Medullary pathology and plaque mapping of these 22 nonbrushite stone formers have been reported previously [2].

### Clinical laboratory studies

Two 24-hour urine samples were collected while patients were on a random diet for measurement of volume, pH, calcium, oxalate, citrate, phosphate, uric acid, sodium, potassium, magnesium, sulfate, and ammonia [4]. We calculated supersaturations with respect to calcium oxalate, brushite, and uric acid using EQUIL 2 [4]. Routine clinical blood samples drawn in the absence of treatments for stone disease served to exclude hyperparathyroidism and overt renal tubular acidosis [5] and to estimate creatinine clearance.

### Biopsy protocol

All ten brushite stone formers underwent PNL for stone removal. Once the collecting system was free of stone and debris, each papillum was visualized using either a rigid or flexible nephroscope. Video footage of each papillum was recorded on S-VHS or DVD format tape and used to evaluate papillary morphology. Subsequently, biopsies were taken from one selected papilla in each of the upper, middle, and lower polar regions of the kidney using a 5 F cup biopsy forceps. At the end of the PNL procedure a biopsy was obtained from the outer cortex using the same biopsy forceps, not necessarily associated with the region of the papillary biopsy. In one patient we were unable to obtain cortical tissue. As we have reported for the prior cases [6] no biopsy site inspected intraoperatively displayed significant hemorrhage, and no postoperative complications related to the biopsy process occurred in any patient. The study was approved by the Institutional Review Board Committee for Clarian Health Partners (#98–073) and conducted according to Declaration of Helsinki principles. Each subject gave informed consent.

### Gross papillary morphology

Using video footage recorded during the PNL access procedure, we evaluated architectural distortions and quantified the area of each papilla covered by pits. Pits are depressions or concavities, usually associated with dilated openings of ducts of Bellini near the papillary tip, but occasionally at the side of a papillary wall. Using the intraoperative recordings [7], total surface area of each papilla was measured, and one of us (J.L.), in a masked manner (i.e., without knowledge of the particular patient),

outlined areas of pitting on one set of prints. The pitted and total papillary areas were converted to numbers of pixels, giving the ratio of pitted to total papillary pixels, or percent coverage with pitted regions.

### Tissue analysis

*General.* Fifty-eight papillary and nine cortical biopsies were studied using light and transmission electron microscopy (TEM). Papillary and cortical biopsy specimens were immediately immersed in 5% paraformaldehyde in 0.1 mol/L phosphate buffer (PPB) (pH 7.4). Four additional papillary biopsy specimens were immersed in 100% ethanol (ETOH). All specimens were refrigerated for three or more days following the initial fixation.

*Light microscopic analysis.* Papillary and cortical biopsies fixed in PPB were dehydrated through a series of graded ethanol concentrations to ETOH prior to embedment in a 50/50 mixture of Paraplast Xtra (Fisher, Itasca, IL, USA) and Peel-away Micro-Cut (Polysciences, Warrington, PA, USA). Papillary biopsies fixed in ETOH were directly embedded in a 50/50 mixture of Paraplast Xtra (Fisher) and Peel-away Micro-Cut (Polysciences). Twelve serial sections were cut at 4 μ and stained with the Yasue metal substitution method for calcium histochemistry [8], hematoxylin and eosin for routine histologic examination or Jones'silver stain for the semiquantitation of glomerulosclerosis. An additional set of serial sections was cut at 7 μ for infrared analysis.

In a double-blind design, two renal pathologists (C.P. and S.B.) performed a semiquantitative analysis on the Jones' silver stained cortical sections from nine of the ten brushite patients, as well as the four controls, 15 calcium oxalate stone formers, and three of the four bypass stone formers from our prior study [2, 3]. Tubular atrophy and interstitial fibrosis were independently scored on a scale of 0 to 3 (0, none; 1, mild or <34% of sample; 2, moderate or 34% to 66%; and 3, severe or >66%). Glomerulosclerosis was defined as increased mesangial matrix with or without wrinkling, thickening and/or collapse of glomerular basement membranes. Sclerosis of individual glomeruli was scored as segmental (<25%, mild; 25% to 75%, moderate) or global (>75%, severe or total obsolescence). The total number of glomeruli observed and the number of glomeruli in each of the three categories of sclerosis were recorded. In all cases, we allowed one degree of grading difference between observers. For greater differences, the tissue was reassessed blindly by offering other sections from the same biopsy to both reviewers.

*Infrared.* We used attenuated total internal reflection (ATR) Fourier transform infrared microspectroscopy (μ-FTIR) to determine the mineral composition of the sites of crystal deposits. Infrared spectra were collected with a Perkin-Elmer Spotlight 300 infrared microscope interfaced to a Perkin Elmer Spectrum One FTIR Spectrometer. The system employed a 100 × 100 μm, liquid nitrogen cooled, mercury cadmium telluride (HgCdTe) detector. The standard germanium internal reflection element was employed in conjunction with a 100 × 100 μ aperture. The ATR method is, in general, an immersion microscopy method, which improves the spatial (x, y, and z) resolution of the microscopic measurement. The combination of the germanium internal reflection element and the aperture yields a 25 × 25 μm sample area. Each spectrum represents the average of 64 individual scans possessing a spectral resolution of 4 $cm^{-1}$. Seven-micrometer thick paraffin sections and standards that included Virginia brushite and calcite (form of calcium carbonate) from Excalibur Mineral Company (Peekskill, NY, USA), calcium oxalate monohydrate from Alfa Products (Danvers, MA, USA), and calcium hydroxyapatite from Spectrum Chemical (Gardena, CA, USA) were analyzed according to our previously published protocol [2].

*TEM.* The 5 mm PPB fixed biopsy specimens of the renal papilla were divided into 1 mm blocks and either routinely processed for TEM or placed in a decalcification solution before embedment. Those tissue blocks routinely processed for TEM were first rinsed in PPB, and then dehydrated through a series of graded ethanol concentrations to ETOH, passed through two changes of propylene oxide before embedment in Epon 812. Those tissue blocks used for decalcification studies were first placed in 0.1 mol/L ethylenediaminetetraacetic acid (EDTA) for 2 months with daily changes of fresh solution and then processed through the ethanol sequence noted above and propylene oxide. Thick sections (~1 μm) were stained with toludine blue, whereas the thin sections (~0.04 μm) were stained with uranyl acetate and lead citrate. All thin sections were examined with a Philips 400 electron microscope.

*Electron diffraction.* The structure of the crystalline material in the papillary tissue of one brushite stone former was determined by TEM electron diffraction. The analysis was performed with a Philips Tecnai 20 at 100 kV and with a diffraction camera length of 890 mm. This sample had been routinely fixed for TEM but not stained.

### Statistics

Twenty-four–hour urine brushite stone former was compared to equivalent measurements from 57 brushite stone formers and 830 calcium oxalate stone formers presented elsewhere [3]. This comparison is not intrinsic to the principal aims of the present work, but is meant to characterize this particular patient group in relation to other larger corresponding groups. For this reason, we simply provide group means, standard errors, and

**Table 2.** Selected laboratory data compared to prior reference populations

| Case | Gender | Serum creatinine *mg/dL* | Serum $CO_2$ | Serum chloride *mEg/L* | Creatinine clearance *mL/min* | Urine pH | Urinary volume *L/24 hours* | Urinary calcium *mg/24 hours* | Urinary citrate *mg/24 hours* | Supersaturation calcium phosphate |
|---|---|---|---|---|---|---|---|---|---|---|
| 1 | F | 0.9 | 28 | 102 | 73 | 5.45 | 0.53 | 250 | 96 | 2.5 |
| 2 | F | 0.7 | 29 | 104 | 144 | 6.12 | 1.8 | 355 | 83 | 2.2 |
| 3 | F | 1.2 | 24 | 106 | 72 | 5.8 | 1.1 | 339 | 160 | 2.6 |
| 4 | M | 1.3 | 26 | 108 | 106 | 6.15 | 1.15 | 166 | 132 | 1.9 |
| 5 | M | 1.3 | 28 | 103 | 77 | 6.46 | 1.45 | 316 | 429 | 3.3 |
| 6 | M | 1.3 | 30 | 100 | 93 | 6.22 | 2.07 | 273 | 62 | 1.6 |
| 7 | M | 0.9 | 27 | 104 | 138 | 5.47 | 1.37 | 380 | 496 | 1.0 |
| 8 | M | 1.1 | 29 | 103 | 94 | 6.67 | 2.63 | 333 | 237 | 1.4 |
| 9 | F | 0.8 | 26 | 106 | 170 | 6.13 | 3.17 | 804 | 1421 | 2.6 |
| 10 | M | 0.7 | 27 | 99 | 233 | 6.22 | 2.37 | 199 | 451 | 0.7 |
| Mean | M | $1.1 \pm 0.1$ | $27 \pm 1$ | $103 \pm 1$ | $123 \pm 23$ | $6.22 \pm 0.2$ | $1.8 \pm 0.2$ | $278 \pm 33$ | $301 \pm 75$ | $1.7 \pm 0$ |
| | F | $0.9 \pm 0.1$ | $26 \pm 1$ | $104 \pm 1$ | $115 \pm 25$ | $5.88 \pm 0.2$ | $1.6 \pm 0.6$ | $437 \pm 125$ | $440 \pm 327$ | $2.5 \pm 0$ |
| Brushite stone formers | M | (1.01–1.11) | (27–28) | (106–108) | (119–140) | (6.2–6.4) | (1.8–2.3) | (295–369) | (407–578) | (2.1–2) |
| | F | (0.79–0.91) | (25–27) | (105–108) | (94–117) | (6.1–6.4) | (1.3–1.8) | (183–273) | (264–494) | (1.5–2) |
| Calcium oxalate stone formers | M | (1.04–1.07) | (27–28) | (106–107) | (125–129) | (5.9–6.02) | (1.67–1.78) | (242–258) | (521–569) | (1.4–1) |
| | F | (0.82–0.86) | (26–27) | (107–108) | (98–106) | (5.9–6.05) | (1.3–1.5) | (190–216) | (476–558) | (1.4–1) |

Abbreviations: Mean, mean values by gender for present cases (± SEM); M, males; F, females. Data from reference populations in parentheses; are shown below the present subjects; brushite stone formers, 40 males and 17 females from prior studies; calcium oxalate stone formers, 625 males and 205 females from prior studies; values for brushite and calcium oxalate stone formers are 95% confidence intervals.

95% confidence intervals for the larger groups and all individual data for the present group, which allows direct inspection and comparison.

Renal cortical pathology was graded as glomerular changes mild, moderate, or severe, and interstitial fibrosis and atrophy. For analysis, we calculated percent of glomeruli with moderate or severe change for each subject (percent glomerular pathology), and added together the scores for interstitial fibrosis and tubular atrophy to give a single score (atrophy/fibrosis score). Using analysis of variance (ANOVA), each score was separately analyzed to evaluate differences between the four groups (brushite, calcium oxalate, bypass, and normal), allowing for age, and number of extracorporeal shock wave lithotripsy (ESWL) treatments, as confounders. The cross product of ESWL and group was estimated to determine homogeneity of slopes for both comparisons. Post hoc analysis of differences between groups for each score was performed using adjusted variables. Conventional software was used (Systat, Point Richmond, CA, USA).

## RESULTS

### Clinical and laboratory characteristics resemble those of other stone former populations

At the time of study patients were 23 to 59 years of age (Table 1). Some had many ESWL, PNL, and endoscopic procedures. Serum creatinine, total $CO_2$, and chloride levels were normal (Table 2). Selected urine chemistries do not differ remarkably from those of our prior 57 brushite stone formers, or our prior 830 calcium oxalate stone formers [3]. The relatively high urine volume and calcium excretions, and low citrate excretions compared to calcium oxalate (Table 2) are as one expects [3].

### Kidney papillae show three kinds of deposits

We observed three patterns of deposit in each of the ten patients. The first pattern is suburothelial white lesions around the openings of ducts of Bellini at the papillary tip (Figs. 1 and 2) that Randall named "type 1" plaque [9]. Such plaque is common on papillae of calcium oxalate stone formers occurs in traces on papillae of nonstone formers, and is an interstitial deposit of apatite particles [2, 9]. The second pattern is large yellow deposits that project from the openings of ducts of Bellini into the urinary space (Fig. 1A and B), and resemble "type 2" Randall's plaque [9, 10]. The third pattern is suburothelial yellow deposits, of variable size, on the sides of papillary tips, away from ducts of Bellini (Figs. 1B and 2A and B). We term these "type 3" for convenience. The larger type 3 deposits are elongate and form a spoke and wheel pattern around the circumference of the papilla, extending from the papillary tip to the fornix (Fig. 2A). Types 2 and 3 deposits were never encountered in calcium oxalate or bypass stone formers, or nonstone former controls [2].

### White and yellow papillary deposits have contrasting histologic characteristics

Type 1 plaque was interstitial apatite deposit (Figs. 1B and 2D) exactly like those we [2] described in calcium oxalate stone formers. This is an expected finding, in that the white suburothelial plaque in these ten patients appeared identical to the white plaque of calcium oxalate stone formers we [2] and others [9–12] have described.

Yellow deposits at the openings of ducts of Bellini (type 2 in this presentation) were crystalline material that completely filled the lumens of ducts of Bellini and associated inner medullary collecting ducts (Figs. 1B and D, 2B and D, and 3A and B). Involved tubules had lumens up to 20

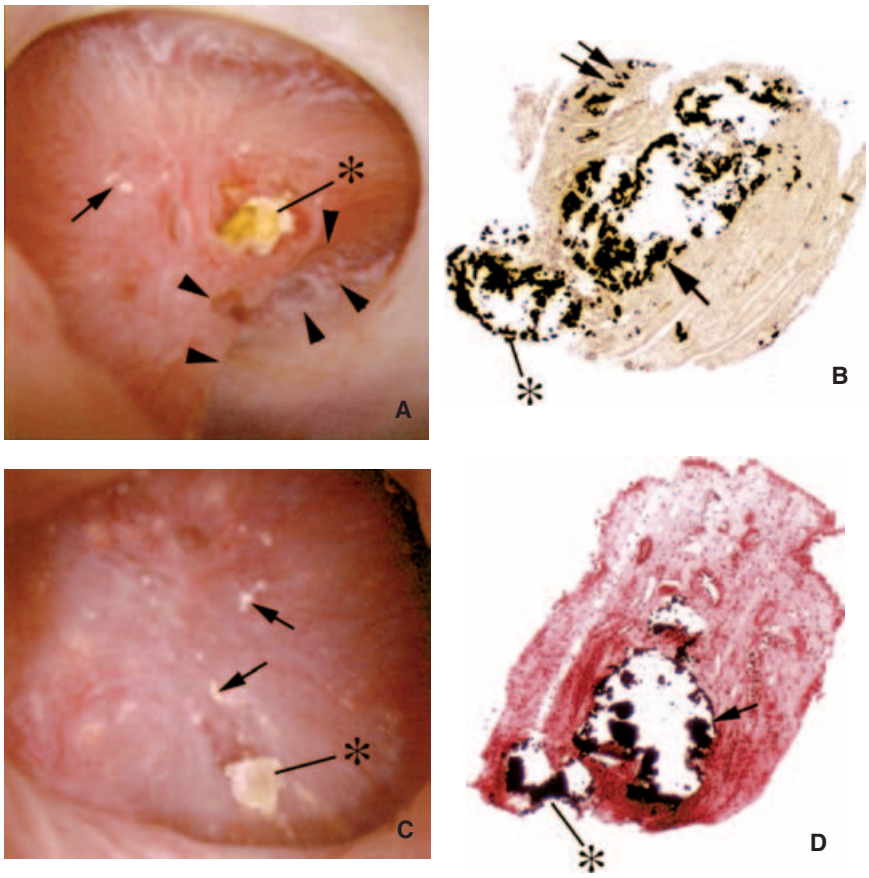


**Fig. 1. Endoscopic (*A* and *C*) and histologic (*B* and *D*) images showing three distinct papillary patterns of crystal deposits in brushite patients.** (A and C) Examples of papilla from brushite patients that were video recorded at the time of the mapping. These papilla show the irregular white areas of crystalline deposits (arrows) (type 1 crystal pattern) beneath the urothelium that we described for calcium oxalate patients. In addition, the papilla from brushite patients possesses sites of a yellowish crystalline deposit at the openings of ducts of Bellini (*) and in a suburothelial location on the sides of the papilla (double arrows). Note the enlargement of the opening of a ducts of Bellini that is filled with crystalline material (*) seen as a depression or "pit" on the papilla. A large pit (arrowheads) is seen along the side of the papilla (A) and does not appear to be associated with a duct of Bellini. (B and D) Low-magnification light-microscopic images of a papillary biopsy specimen from a brushite patient are shown; the sites of calcium deposits were stained black by the Yasue metal substitution method for calcium histochemistry. An enormous amount of Yasue-positive material is seen with ducts of Bellini (arrows). This crystalline material is seen protruding from the opening of the duct of Bellini and also in an associated inner medullary collecting duct (*). In addition, Yasue-positive material (B) is in the interstitium of the renal papilla surrounding thin loops of Henle (double arrows) as we have previous described for calcium oxalate stone formers [magnification ×90 (B); ×100 (D)].

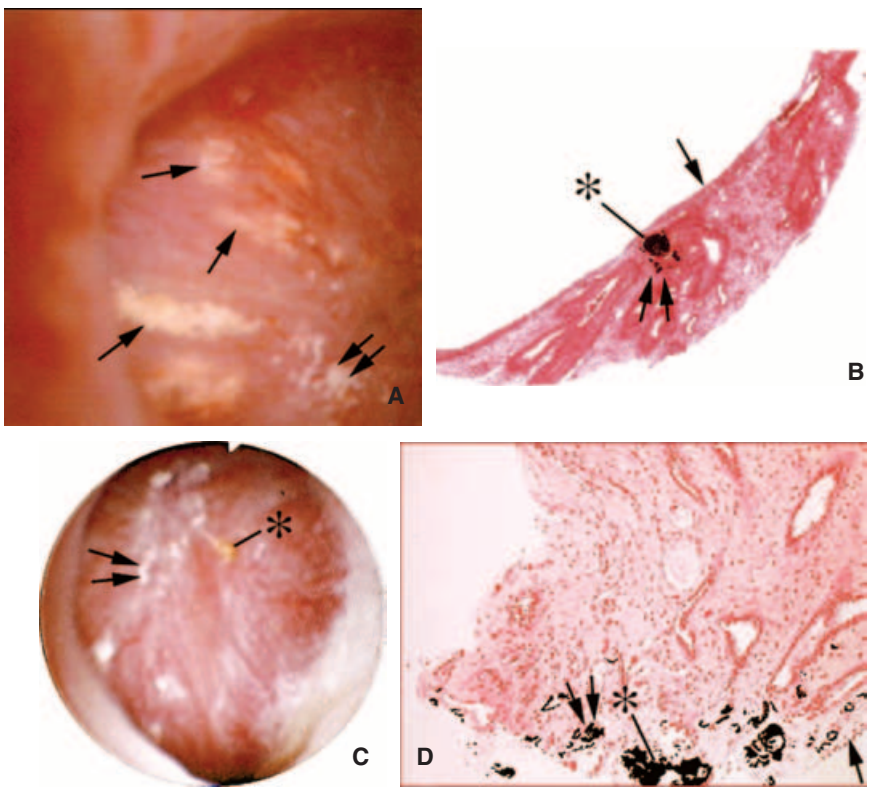


**Fig. 2. Endoscopic (*A* and *C*) and histologic (*B* and *D*) images showing the third (type 3) pattern of crystal deposits in papillary biopsies from two brushite patients**. During endoscopic examination of the renal pelvis, this pattern of yellowish mineral deposition is found within lumens of medullary collecting ducts just like that described for the type 2 pattern, except that these collecting ducts are located just beneath the urothelium. Sites of deposit ranged from large areas of crystal deposition in collecting tubules that formed a spoke and wheel-like pattern around the circumference of the papilla (A) (arrows) to small, single sites of yellowish material in focal regions of a collecting duct lumen (C) (*). The papilla (A and C) also show the type 1 pattern of whitish crystal deposition that correlate with interstitial sites of Randall's plaque (double arrow). Histologic analysis of the type 3 deposits (B) confirms that these sites of crystal deposition are in medullary collecting ducts (*) positioned just beneath the urothelium lining (arrow) of the renal pelvis (A and B). The collecting ducts (A) are filled with crystalline material as revealed by the Yasue stain. (B and D) Yasue-positive material is noted in the interstitium adjacent to thin loops of Henle (double arrow) [magnification ×250(B); ×700 (D)].

times their normal diameter (Figs. 1A, 2B, and 3A and B), and only a few of the most enlarged tubules were detected in any one biopsy. The openings of involved ducts were greatly enlarged and filled with crystalline material that projected into the urinary space (Fig. 1). Some of the dilated inner medullary collecting ducts extended from the papillary tip toward the outer medulla (Fig. 3C and D).

Type 3 yellow suburothelial deposits along the sides of papillae were outer and inner medullary collecting duct near the surface of the papilla but not at the point of tubule fluid egress from Bellini ducts (Figs. 2 and 3). In other words, yellow deposits were always crystal masses in collecting duct lumens that differed in geometry because one is localized in Bellini ducts while other involves longer lengths of inner and outer medullary collecting ducts.

### Renal papillary cells are abnormal

*Tubule cells.* Some tubules altogether lacked viable cells. Cells lining collecting ducts with deposits varied from irregular shape to complete loss (Fig. 4). Some cells, all dead, were filled with mineral deposits (Figs. 4 and 5). Other cells were coated with crystals imbedded in membrane proteins or proteins coating the cell surfaces. Many coated cells appeared viable, but none had normal morphology (Fig. 5). In particular, nuclei were normal, and no evidence of apoptotic changes were observed. In the absence of crystals, collecting ducts cells were invariably normal.

*Interstitium.* Cuffing of fibrosis, without chronic inflammation (Fig. 1B and D) surrounded individual isolated collecting ducts with deposits in them. Multiple adjacent collecting ducts contained crystals and ducts were embedded in large fields of fibrosis containing chronic inflammatory cells (Figs. 3 and 4). In such regions of dense fibrosis, thin loops of Henle and vasa recta were injured as indicated by loss of lining cells, greatly thickened basement membranes, and narrowed tubular lumens (Fig. 4). Interstitium around normal collecting duct was without pathologic change.

### Papillary pitting reflects dilated ducts of Bellini

Individual papilla often showed depressions (pitting) near the papillary tip, a phenomenon not observed in calcium oxalate or bypass stone formers. These depressions or concavities were usually near the openings of ducts of Bellini that contained crystalline material (Fig. 1A and C). Histologically, such pits are hugely dilated lumens of Bellini ducts, enlarged as much as 20 times above normal by enormous intratubular crystal deposits. In other words, pitting is part of type 2 deposits. Occasional pits invaded the sides of a papillary wall and were not associated with a duct of Bellini (Fig. 7A). Their histology is not yet defined.

### Pitting, deposits, epithelial cell damage, and interstitial changes are parallel

*Pitting.* Because it is the two kinds of pitting that distort the regular conical shape of the papilla, percent of papillary pitting is a quantitative gauge of architectural distortion. Cases 1, 2, 4, 7, and 8 showed a minimal amount of papillary pitting at 0%, 0.2%, 0.4%, 0.2%, and 0.2%, respectively. Figure 6 shows all of the papilla (except the lower lateral papilla which could not be accessed) from case 1. No evidence of papillary deformity is noted. Cases 3, 5, 6, and 9 showed more extensive papillary pitting at 6%, 3.7%, 21.1%, and 25.7%, respectively. Figure 7 shows all the papillae from case 5 and that the majority are deformed. Case 10 showed an intermediate level of pitting at 1.6% (not illustrated). These rather coarse groupings of stone formers by percent pitting have a robust relationship to the degree of histologic abnormality.

*Tubule changes.* Although all ten patients had some tubule crystal plugging, the extent and severity varied from case to case. Renal tissue from cases 1 and 7, who had minimal pitting, showed normal inner medulla punctuated by occasional plugged individual collecting duct segments (Fig. 2C and D). In cases 3, 5, 6, and 9 whose pitting was more marked, numbers of adjacent tubules were involved (Fig. 3A and B), not only collecting duct, but also nearby thin loops of Henle, that were never involved in cases 1 and 7. Moreover, tubule plugging extended into the outer medulla, a region not involved in any of our other biopsies (Fig. 3C).

*Interstitial changes.* Cases 1 and 7, with minimal lesions, showed infrequent interstitial fibrosis around solitary enlarged collecting duct filled with crystals (Fig. 2D). In cases 3, 5, 6, and 9, large regions of interstitial fibrosis engulf numerous tubules (Fig. 4A and B). The fibrosis expands well beyond the immediate neighborhood of plugged tubules and surrounds thin loops of Henle that do not contain crystal plugs. Because we never find interstitial disease in the absence of collecting duct injury, and interstitial disease is roughly parallel to collecting duct deposits and injury, we infer that interstitial changes are a response to collecting injury and not themselves a primary process.

*Intermediate grades of severity (cases 2, 4, 8, and 10).* In cases 2, 8, and 10 some regions contained mild lesions of isolated plugged collecting ducts surrounded by focal interstitial fibrosis, and other regions contained the severe lesions of multiple adjoining plugged collecting duct with extensive interstitial fibrosis. In other words, their lesions spanned the range of severity we have encountered, whereas cases 3, 5, 6, and 9 had severe lesions everywhere we sampled, and cases 1 and 7 had only mild

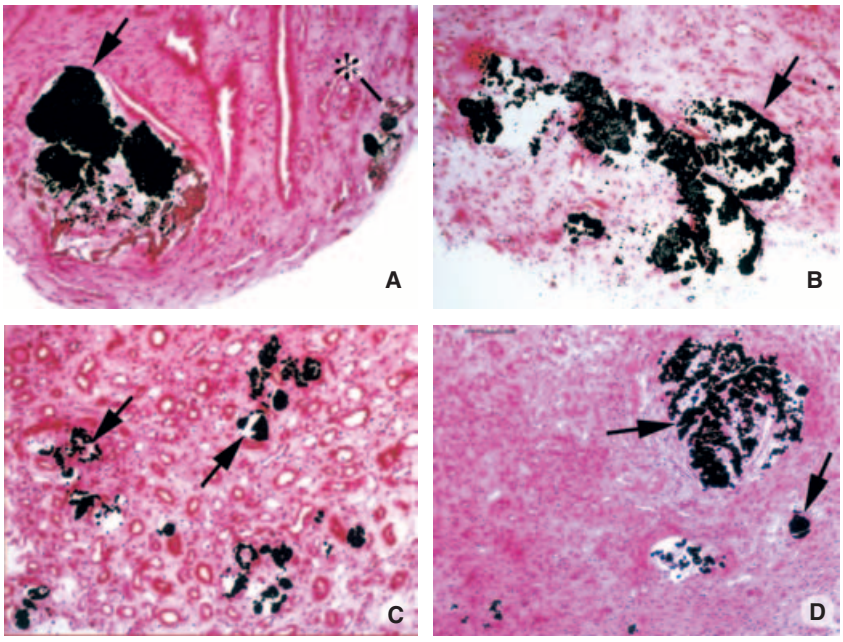


**Fig. 3. Crystal deposition seen by light microscopy localized to collecting ducts of the inner (*A* and *B*) and outer (*C* and *D*) medulla.** (A and B) Yasue-positive material is seen localized in individual to a small group of inner medullary collecting ducts (arrows) and occasionally nearby loops of Henle while nearby duct appear normal (*). The crystalline material greatly expands the tubular lumen of these tubules. (C and D) Yasue-positive material is seen extending into the outer medulla where the crystalline materials is found in the lumens of outer medullary collecting ducts (arrows) but in a focal manner such that these crystalline tubules are surrounded by many normal appearing tubules (magnification ×700).

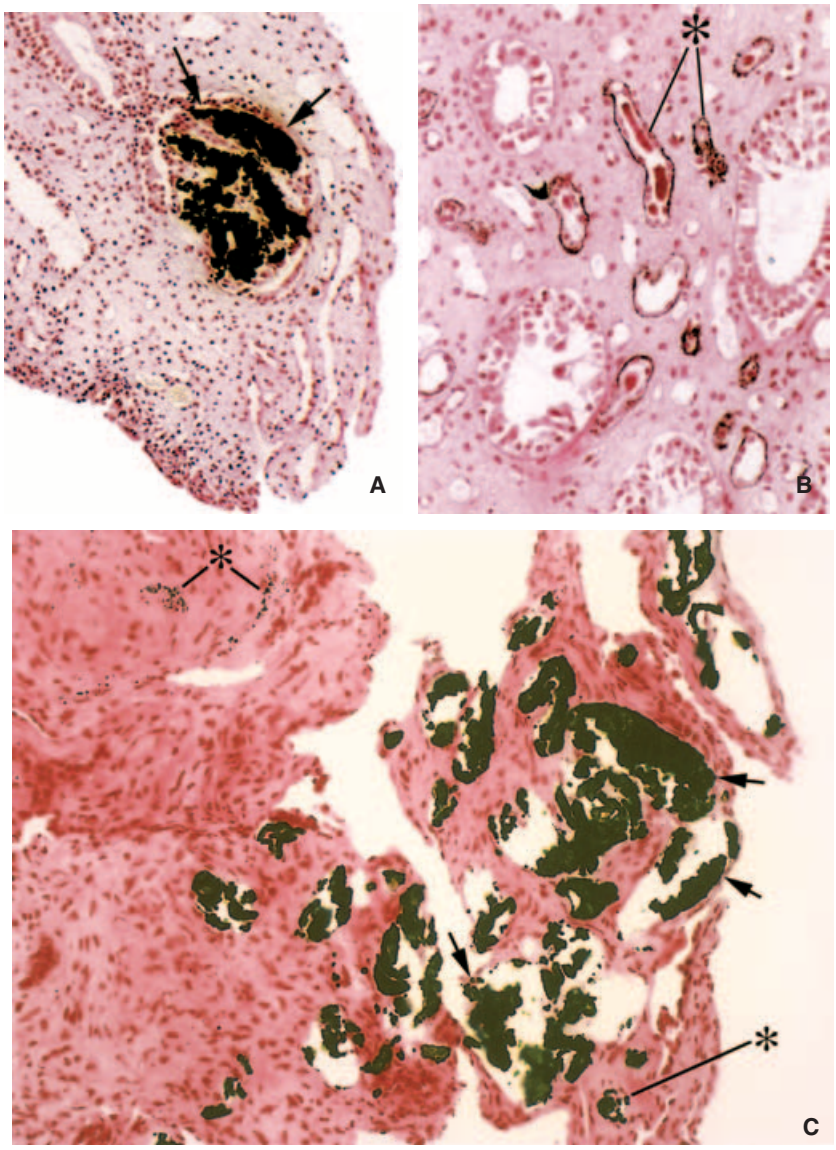


**Fig. 11. A comparison of histopathogy of parallel tissue samples from patient 10 fixed in 100% ethanol (ETOH) (*A* and *B*) or 5% paraformaldehyde in phosphate buffer (PPB) (pH 7.4) (*C*).** Crystal deposition was identical in location for both fixatives. Distinct crystals were noted in the basement membranes of thin loops of Henle (*) (B and C) and in the lumens of medullary collecting ducts (A and C, arrow) (magnification ×900).

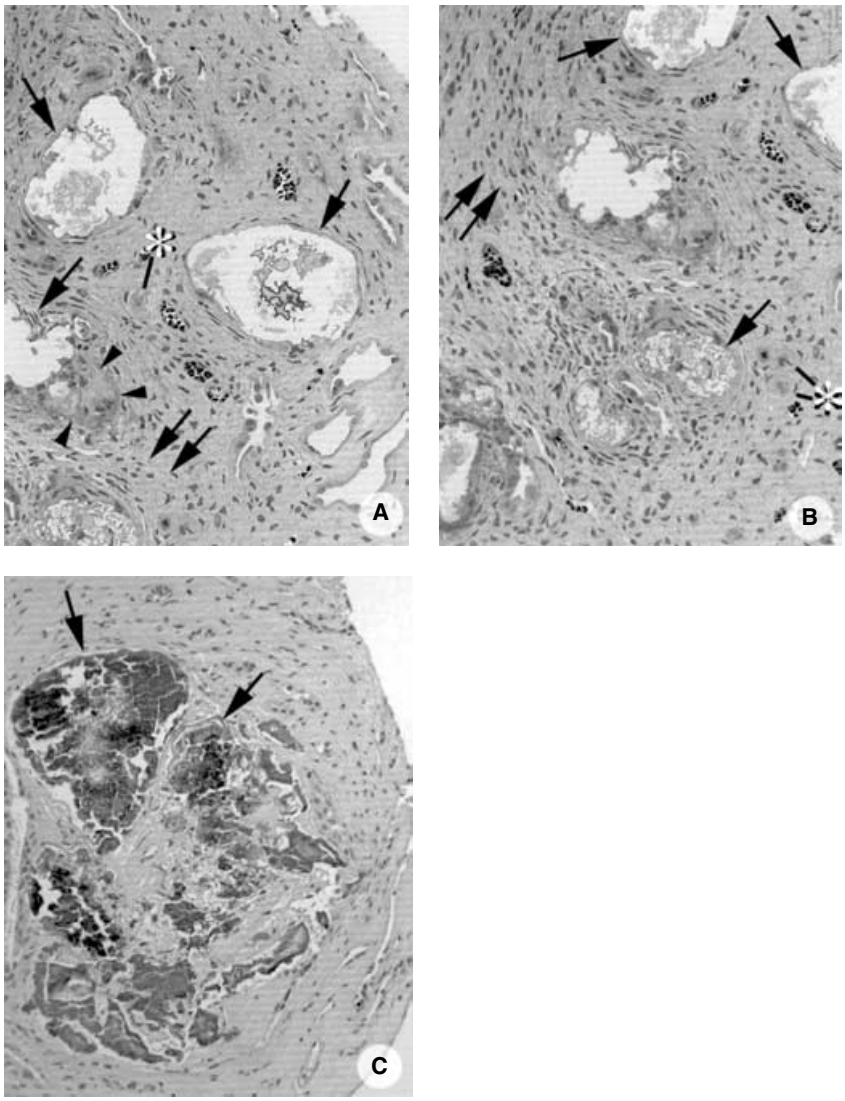


**Fig. 4. Interstitial changes accompany severely injured crystal filled collecting ducts.** All three of these light microscopic images were obtained from 1μ thick plastic histologic sections of papillary biopsies from our brushite patients. The tissues (*A* and *B*) were decalcified with 0.1 mol/L ethylenediaminetetraacetic acid (EDTA) for 2 months so that the cellular detail of the crystalline-filled tubules could be more easily analyzed while (*C*) is from a calcified biopsy. (A and B) Extensive cellular damage is noted in several inner medullary collecting (arrows) where the mineral had being chemically removed. These images were obtained from a papillary biopsy collected from patient 6 where the gross morphology of all papilla was severely injured. Extensive regions of interstitial fibrosis surround the injured collecting tubules (double arrows). Entrapped injured thin loops of Henle and vasa recta (*) are also noted in these fields of interstitial fibrosis. (C) A series of crystalline-filled collecting tubules (arrows) that are embedded in a small ring of fibrosis tissues. This tissue was not decalcified so regions of mineral deposition are easily seen in this hematoxylin and eosin stained section. Normal tubular profiles are seen adjacent to these injured collecting tubules. This sample was obtained from case 4. An occasional giant cell (arrowheads) was observed near damaged collecting ducts as seen in (A) (magnification ×1100).

lesions. In case 4 all lesions were mild, but all papillae were abnormal, and lesions involved every region we sampled (Fig. 3D). In other words, inspection of disease of intermediate severity supports our findings derived from an inspection of extremes and suggests that our basic sequence of pathogenesis from collecting duct damage to interstitial fibrosis is not unreasonable.

### Cortical changes are more marked in brushite than other patients

Glomerulosclerosis had progressed to moderate or global change in eight of the nine brushite stone formers (Table 3). By contrast, intestinal bypass stone formers had only mild to moderate levels of glomerular pathology, and only half of the calcium oxalate stone formers, and controls, showed any evidence of glomerulosclerosis, never of more than mild degree. All brushite stone formers displayed some tubular atrophy that was advanced in six of nine. The controls, calcium oxalate, and intestinal bypass stone formers showed a minimal level of tubular atrophy. No cortical interstitial changes were noted in the controls. The calcium oxalate and intestinal bypass stone formers possessed a minimal degree of cortical fibrosis. In marked contrast, all brushite stone formers had moderate to severe cortical fibrosis. Although of equivalent age, and reasonably balanced gender ratios, the brushite stone formers harbor a significant level of cortical pathology, with overt nephron loss, whereas cortical changes in calcium oxalate and bypass stone formers are more muted, and controls almost none.

Cortical and papillary changes were not always parallel in the brushite stone formers. For example, case 1, with mild papillary pathology had moderate cortical disease. Case 2 had severe cortical pathology with intermediate papillary pathology. Serum creatinine levels (Table 2) and creatinine clearance values by no means paralleled cortical changes. Whereas papillary deposits, collecting

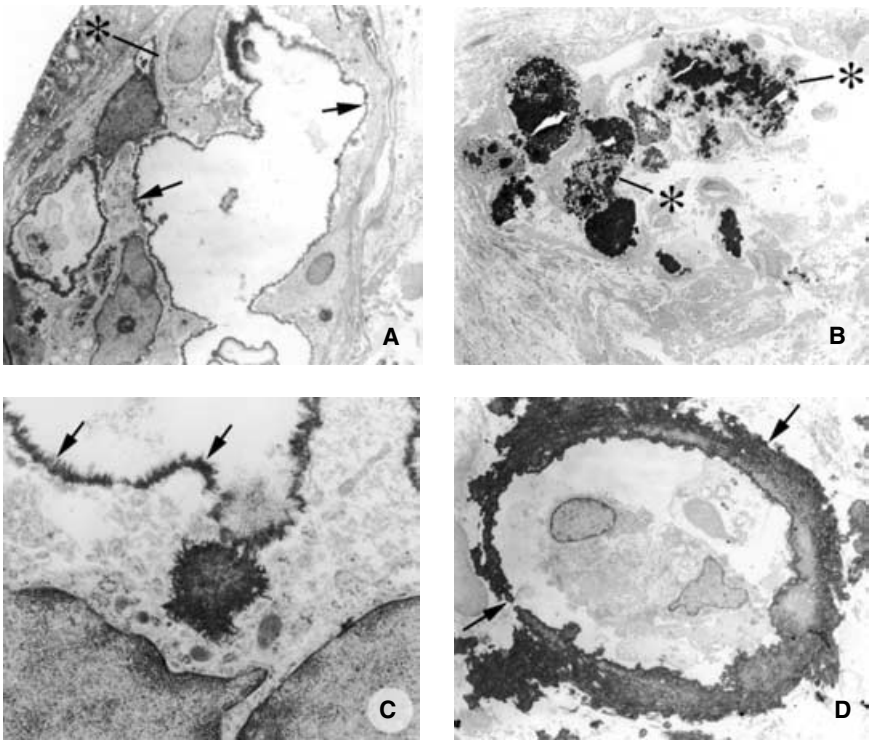


**Fig. 5. Transmission electron microscopic (TEM) changes in crystal-filled collecting ducts.** (*A* and *B*) Sections were obtained from a papillary biopsy from case 6. (*C* and *D*) Sections were obtained from a papillary biopsy from case 1. (A) The lining cells (*) of this decalcified inner medullary collecting tubule are covered by an electron dense matrix material (arrows). A similar area of matrix (arrows) covering the apical cell surface is seen at a higher magnification (*C*). The tubular cells (A) are highly irregular in shape while the cells (B) are filled with crystal deposits (*) and show evidence of injury. (*D*) A ring of crystalline material (arrows) is seen filling the basement membrane and surrounding the basal surface of a thin loop of Henle, a pattern typical of calcium oxalate stone formers [magnification ×2800 (A); ×100 (B); ×13000 (C); and ×2800 (D)].

duct cell injury, and interstitial fibrosis seem closely related, the cortical and papillary abnormalities seem less so, perhaps because the sampled regions of cortex are not drained by the sampled regions of papilla.

### Statistical analysis of group differences

The foregoing qualitative description of changes in renal cortex can be further quantified by combining atrophy and fibrosis into a single score that depicts interstitial disease (atrophy/fibrosis), and using percent of glomeruli with moderate or severe changes as a score for glomerular disease (percent glomerular pathology) (see the **Methods** section).

*Atrophy/fibrosis.* Brushite stone formers had grossly higher scores (4.1 ± 0.3 vs. 1.4 ± 0.3, 1.3 ± 0.6, and 0, brushite vs. calcium oxalate, bypass, and control, respectively) than the other three groups (Fig. 8A). Brushite patients also had more ESWL procedures (3.7 ± 1.0 vs. 0.4 ± 0.1, 2.0 ± 2.0, and 0, brushite vs. calcium oxalate, bypass, and control, respectively) (Fig. 8C). To evaluate the hypothesis that the higher atrophy score in brushite stone formers is due to their larger number of ESWL procedures, we performed ANOVA with the score as dependent and ESWL and age as covariates. Age was not significant ($P = 0.64$), ESWL was marginally significant ($P = 0.059$), and the adjusted score of brushite stone formers exceeded that of calcium oxalate stone formers (3.7 ± 0.4 vs. 1.7 ± 0.3) ($P = 0.001$) and also exceeded 0, the score for controls ($P < 0.001$) and that for bypass (1.1 ± 0.6) ($P = 0.001$). Even though brushite stone formers had more ESWL procedures, ESWL is not sufficient to account for the higher atrophy/fibrosis score compared to the other three groups. Homogeneity of slopes was present for ESWL.

*Percent glomerular pathology.* Brushite stone formers had a higher percent glomerular pathology score than the other three groups (45 ± 11 vs. 5 ± 4, 11 ± 11, and 0, brushite, calcium oxalate, bypass, and control, respectively) (Fig. 8B). By ANOVA with percent pathology as dependent, age and ESWL as covariates, neither age nor ESWL were significant confounders ($P = 0.74$ and $P = 0.80$, respectively). Brushite stone formers glomerular score exceeded that of all three other groups ($P = 0.001$, $P = 0.03$, and $P = 0.001$, calcium oxalate, bypass, and control, respectively). Unlike atrophy/fibrosis, glomerular injury was not related to ESWL, but was higher in brushite stone formers than the other groups (Fig. 8C).

### The crystal deposits are composed of apatite

μ-*FTIR analysis.* Yasue-positive deposits in the tubular lumens of medullary collecting ducts and the interstitium around the thin loops of Henle of all ten brushite stone formers showed primary spectral bands for hydroxyapatite and calcium carbonate in both PPB- and ETOH-treated biopsies (Fig. 9). Spectra from deposits and the hydroxyl apatite reference material correspond. The reference material (calcium hydroxyapatite) (Spectrum Chemical, Gardena, CA, USA) has a small amount of calcium carbonate reflected in the presence of bands

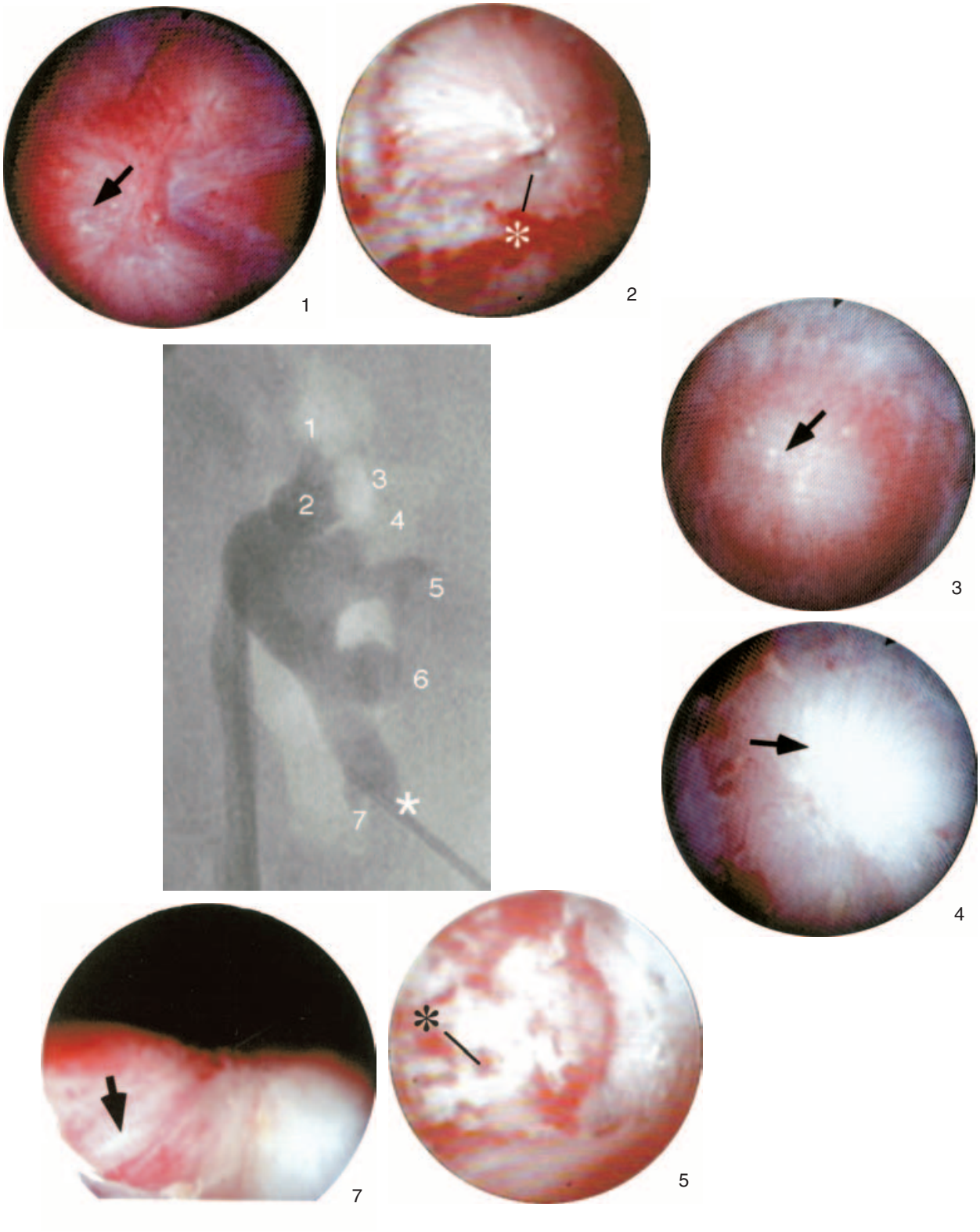


**Fig. 6. Endoscopic images showing gross morphology of renal papilla of brushite case 1.** In the center is an x-ray image of the entire collecting system with each calyx numbered starting at the upper pole. The gross morphology of individual papilla from this brushite patient that was video recorded at the time of the mapping is shown. Papilla 1, 3, 4, and 7 are normal appearing in that no sites of deformations (pitting) were seen. These papilla do show sites of suburothelial white deposits (arrows) we have noted present in calcium oxalate stone patients. In papilla 2 and 5, a few shallow pits (*) are seen near the papilla tip. The asterisk denotes the papilla used to indicate access.

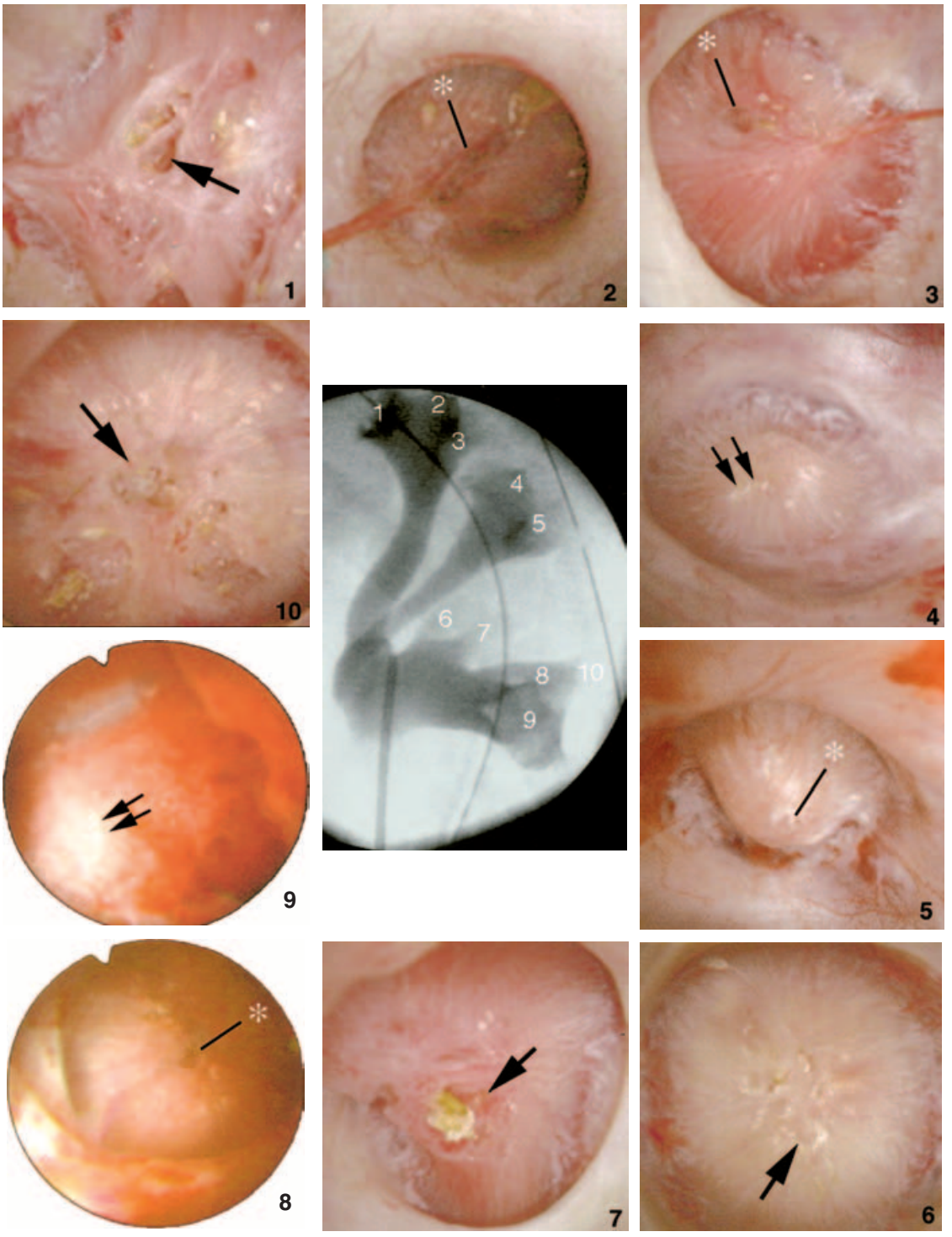


**Fig. 7. Endoscopic images showing gross morphology of renal papilla of brushite case 5.** In the center is an x-ray image of the entire collecting system with each calyx numbered starting at the upper pole. The gross morphology of individual papilla from this brushite patient show greater amount of pitting across much of the papillary surface and more of the papilla are involved than that documented in case 1 (Fig. 6). Papilla 1, 6, 7, 8, and 10 show severe pitting (arrows) while papilla 2, 3, and 5 show fewer pits (*). Papilla 4 and 9 only show sites of Randall's plaque (double arrows).

located near 1400 and 870 $cm^{-1}$. These features are not typically observed in spectra of natural hydroxyapatite.

Electron diffraction analysis identified as biologic hydroxyapatite (Fig. 10), the crystal deposits in the tubular lumens of brushite case 5. The electron diffraction pattern shows the sharp 002 diffraction peak reflecting the elongated nature of the crystals and the broad diffraction band containing the 211, 112, and 300

**Table 3.** Cortical pathology of stone formers

| Age | Glomeruli | Glomerular pathology | | | Tubular atrophy | Interstitial fibrosis |
|---|---|---|---|---|---|---|
| | | Mild | Moderate | Global | | |
| Calcium oxalate | | | | | | |
| 30 | 2 | | | | 1 | 1 |
| 63 | 1 | | | | 1 | 1 |
| 44 | 20 | | | | 1 | 1 |
| 53 | 21 | | 9 | | 2 | 2 |
| 58 | 16 | 2 | | | 1 | 1 |
| 74 | 18 | 1 | | | 1 | 1 |
| 24 | 6 | | | | 1 | 1 |
| 41 | 10 | | | | 0 | 0 |
| 29 | 2 | | | | 0 | 0 |
| 46 | 1 | | | | 0 | 0 |
| 27 | 9 | | | | 1 | 1 |
| 48 | 13 | 2 | | | 1 | 1 |
| 61 | 5 | | 2 | | 1 | 1 |
| 53 | 6 | 1 | | | 0 | 0 |
| 75 | 22 | 4 | | | 0 | 0 |
| Brushite | | | | | | |
| 42(1) | 28 | | 19 | | 2 | 2 |
| 42(2) | 59 | | | 59 | 3 | 3 |
| 59(3) | 17 | | 6 | | 2 | 3 |
| 23(4) | 17 | | 6 | | 1 | 3 |
| 42(5) | | | | | | |
| 64(6) | 11 | | 6 | | 2 | 2 |
| 52(7) | 15 | 3 | | | 1 | 2 |
| 31(8) | 24 | | 1 | | 2 | 2 |
| 44(9) | 11 | | 3 | | 2 | 2 |
| 39(10) | 11 | | | 9 | 1 | 2 |
| Control | | | | | | |
| 40 | 29 | 1 | | | 0 | 0 |
| 52 | 65 | | | | 0 | 0 |
| 41 | 100 | | | | 0 | 0 |
| 71 | 70 | 1 | | | 0 | 0 |
| Bypass | | | | | | |
| 52 | 9 | 1 | | | 1 | 1 |
| 49 | 27 | | 9 | | 0 | 0 |
| 61 | 4 | 1 | | | 1 | 1 |

Abbreviations: Age, age at papillary biopsy; case number for brushite stone formers in parentheses; Control subjects; bypass, patients with stones due to intestinal bypass for obesity; number in parentheses are from a previous report; glomeruli, number of glomeruli in sample; glomerular pathology, findings about glomeruli, reported as number of glomeruli in sample showing mild moderate or global changes (see **Methods** section); blank, no glomeruli show the changes for that column; tubular atrophy, and interstitial fibrosis are graded in a scale of 0 to 3 intensity units as noted. Note that cortical tissue was not obtained in one instance [42(5)] above.

diffraction peaks that are characteristic of biologic apatite [13].

### Crystals are not an artifact of PPB

Parallel tissue samples from case 10 were fixed both using 5% paraformaldehyde in 0.1 mol/L PPB, and ETOH. The μ-FTIR analysis (Fig. 9) of intratubular crystal deposits in parallel sections gave identical spectra from PPB- and ETOH-fixed tissues. Similarly, Yasue-stained sections from the same parallel tissue samples fixed in either PPB or ETOH showed identical patterns of crystal deposition in the basement membrane of thin loops of Henle and at sites of tubule plugging of medullary collecting duct (Fig. 11). These findings make improbable the speculation that PPB itself created the crystallizations we have observed. Since spectra from PPB- and ETOH-fixed tissues give identical results, it is also difficult to maintain that PPB produced the apatite we have observed, or modified the crystal structure.

## DISCUSSION

### Brushite stone formers have a papillary lesion not hitherto described

To date, the combination of interstitial apatite plaque and apatite plugging of collecting duct with cell death and interstitial fibrosis has not been described. Calcium oxalate stone formers have interstitial apatite plaque of a magnitude like that of the brushite stone formers, but no collecting duct deposits [2]. Our four intestinal bypass stone formers [2] all had apatite plugging of collecting ducts, but no interstitial plaque. Their collecting duct lesions were minor compared to brushite stone formers, whose papillary lesions involve more tubules, larger masses of crystal, a greater dilation of collecting duct lumens, greater lengths of the renal papillum, more cell death, and more extensive and severe interstitial inflammation and fibrosis. Perhaps for this reason, we did not find gross distortions of papillary architecture in the bypass patients, as we did here. In other words, brushite stone formers combine the apatite plaque of calcium oxalate stone formers and the collecting duct lesions of bypass stone formers in a severe form.

### Thus far, only brushite stone formers have significant renal cortical disease

In addition to severe papillary disease, brushite stone formers have more glomerulosclerosis, tubular atrophy, and interstitial fibrosis than calcium oxalate and bypass stone formers of similar age (Table 3). Clinical measures might not alert clinicians to the nephron loss that cortical pathology connotes; creatinine clearances of cases 1, 3, 4, 5, 6, and 8 are low compared to calcium oxalate stone formers and 1, 3, 4, 5, and 6 are low compared to our pool of brushite stone formers (Table 2); others are normal. The mean values by gender for our present ten patients are within the 95% CI for our brushite stone formers pool. The mean creatinine clearance for the six present male patients is below the mean for our pool of calcium oxalate stone formers, while the female mean is within the 95% CI for our female calcium oxalate stone formers. As expected serum creatinine levels of our present cases show corresponding elevations. Creatinine clearance can over estimate true glomerular filtration rate because of creatinine secretion by renal tubule cells [14], and hyperfiltration by remaining nephrons can obscure the reduction of nephron number. Without biopsy, the extent of renal damage cannot be gauged. We do not advocate biopsy of brushite stone formers, but point out the presence of a renal disease that requires additional study.

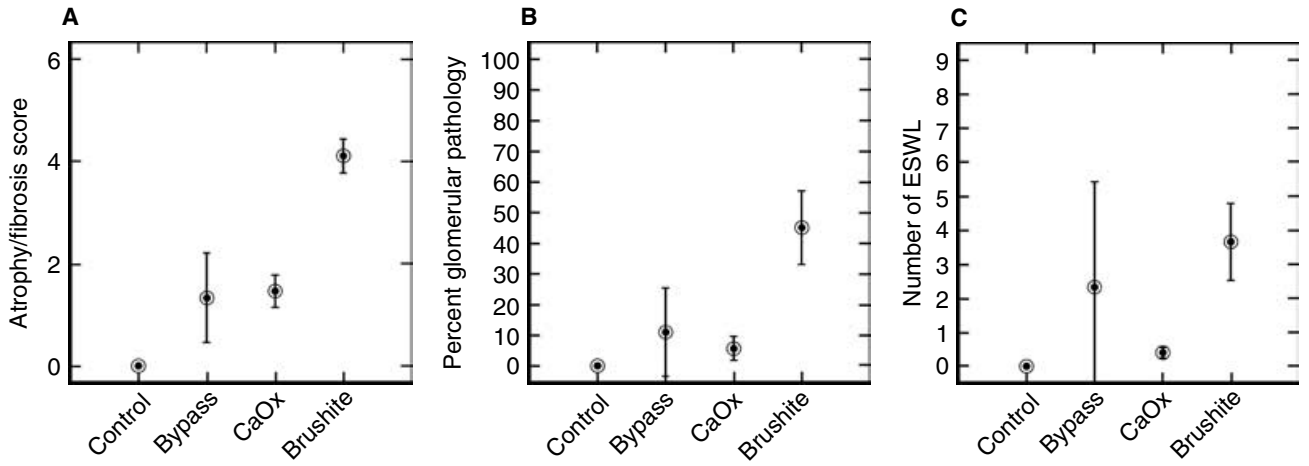


**Fig. 8. Cortical changes and extracorporeal shock wave lithotripsy (ESWL) procedures.** Brushite stone formers had higher cortical atrophy/fibrosis scores (*A*) and percent of glomeruli (*B*) with pathologic changes than controls or calcium oxalate or bypass. They had more ESWL procedures than controls or calcium oxalate stone formers (*C*). Values are mean ± SEM.

## Histologic changes support a preliminary pathogenetic scheme

In no instance did we find collecting duct epithelial cell changes in the absence of crystals, or interstitial changes in the absence of collecting duct cell changes. Moreover, we never found crystal deposits without some cell abnormality adjacent to the deposits. Cells coated with crystal are viable but deformed; those containing crystals are always dead. Because we never found a viable cell containing internalized crystals, we propose but cannot prove that crystals entered these cells after death. Therefore, it is not unreasonable to infer a provisional pathogenetic sequence: (*1*) crystallization in collecting duct; (*2*) crystals contact collecting duct cells; (*3*) cells are injured; (*4*) some collecting duct cells die; (*5*) crystallization and cell loss progress to greatly enlarged collecting ducts in the extreme case; (*6*) interstitial inflammation is provoked around injured collecting duct cells; and (*7*) renal tissue is sequentially involved. Initial scattered terminal collecting duct plugging is followed by progressive involvement of medullary structures, including collecting duct, interstitium, vas recta, and thin loops of Henle. Since we never find cell injury or change without crystals, it is difficult at this time to propose that cell injury precedes crystallization, but there is a caveat: loss of normal pH regulation in a collecting duct, from obstruction, or other causes could trigger crystal formation yet not manifest histologically.

The cortical changes, being separate, are of less certain origin. We propose they may arise from intranephronal obstruction by crystal deposits and cell damage in the remarkably strategic locale of the terminal collecting duct. Only 100 or so Bellini ducts drain the 1 million nephrons of each human kidney [15], and there are no anatomic bypass systems around a blocked duct. The nonspecific cortical changes are compatible with this hypothesis. Chronic obstruction can lead to exactly this picture [16, 17]. To test this hypothesis in human tissue would require we demonstrate some sequence of changes specific to obstruction, a matter beyond the present work. Of clinical note, the nonspecific pattern of cortical renal injury could be deceptive if a patient presented with chronic renal failure. Before this work, no one would consider a past history of stones as germane to renal disease with cortical scarring. Of course, at this stage, we cannot state that these patients in particular will have the propensity to progress to chronic renal failure.

## Others have described similar but not identical pathology

The closest example to the brushite lesion that we could find is yellow deposits in medullary collecting duct in a single individual with acute lymphatic leukemia and uric acid nephropathy [18]. Uric acid–plugged tubules lost lining cells, and nearby interstitium was scarred. Occasional urate crystals were seen in the interstitium associated with giant cells. Secondary lesions included dilation of medullary collecting duct, tubular atrophy, and cortical scarring. At the papillary tip linear yellow striations termed "uric acid infarct" extended from the papillary tip to the renal fornix. These striations were thought to represent large amounts of urate and calcium deposits in medullary collecting duct. Renal cortical changes associated with distal obstruction of the nephron have been reported in these patients. This lesion differs from brushite stone formers in lacking apatite interstitial plaque, and, of course, in the nature of the crystals involved. It occurred as a consequence of leukemia.

Patients deficient in adenine phosphoribosyltransferase [19] obstruct their medullary collecting duct and other tubule segments with deposits of DHA (2,8-dihydroxyadenine) crystals. All sites of crystal deposits are associated with progressive cellular damage and

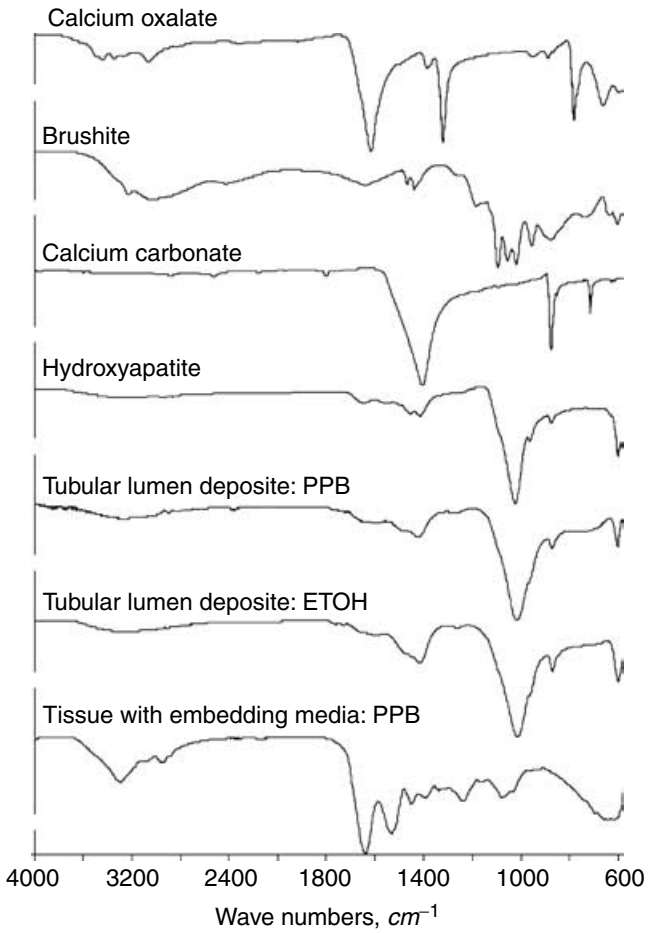


**Fig. 9. Fourier transform infrared microspectroscopy (μ-FTIR) spectra of crystal deposits from the brushite patients.** A series of infrared attenuated total internal reflection (ATR) spectra were obtained for a set of standards (calcium oxalate, brushite, calcium carbonate, and hydroxyapatite) for a site of calcium deposition (Yasue-positive area) in the lumen of a inner medullary collecting duct of a brushite patient fixed in the 5% paraformaldehyde in phosphate buffer (PPB) (pH 7.4), or 100% ethanol (ETOH), and for the tissue sample fixed in PPB with embedding media from case 10. The infrared spectra of the Yasue-positive areas show a spectral band for hydroxyapatite. About a half of the Yasue-positive areas in tubular lumens also showed a spectral band for calcium carbonate.

atrophy. Tubular degeneration, inflammation, interstitial fibrosis, and tubular atrophy extend from the renal medulla to the renal capsule. Like uric acid nephropathy in the leukemia patient, this is an instructive if somewhat different situation. The crystallization occurs in many sites. Being multifocal rather than mainly papillary, it is not so close a match as the uric acid lesion in the leukemia patient.

Altogether, the lesions we describe in brushite stone formers do not have an exact counterpart. Neither of the two instances noted above bear anything but a superficial resemblance. Brushite nephropathy is a chronic papillary and cortical disease of a particular kind of calcium stone

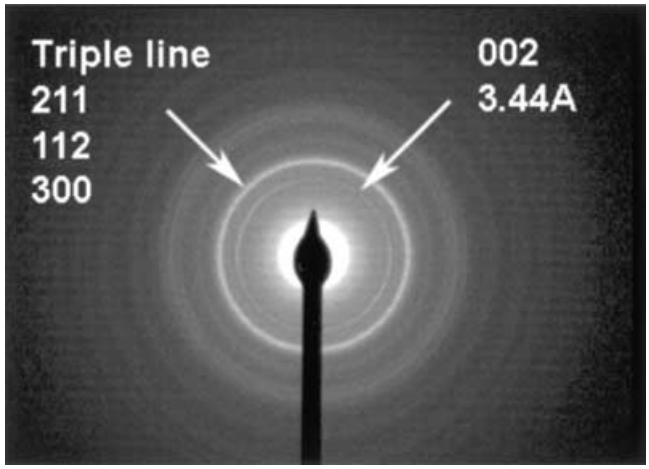


**Fig. 10. Transmission electronic microscopic (TEM) electron diffraction pattern of crystalline deposits in a brushite patient.** An area of intratubular crystal deposition from case 5 was analyzed by electron diffraction and identified the crystalline material as biologic hydroxyapatite. It shows the sharp 002 diffraction peak reflecting the elongated nature of the crystals and the broad diffraction band containing the 211, 112, and 300 diffraction peaks which is a characteristic of biologic apatites.

former. We believe it is hitherto undescribed in its complete form.

### Crystal deposits are not an artifact of tissue preparation

We recognize that because our routine tissue fixation solution uses a 0.1 mol/L PPB, one could speculate that the buffer itself caused the crystallizations we present here. To make certain about buffer artifact, we preserved parallel tissue samples in buffer and in 100% ETOH, a fixative that gives inferior histologic results, but avoids the PPB. Results are definitive in that localization of crystals, mass of crystals, and infrared spectra of crystals are the same with buffer and ETOH fixation, excluding buffer as the source of the deposits.

### Surgically observed lesions have specific histologic counterparts

During PNL in 15 calcium oxalate stone formers [2], four controls, and the present ten brushite stone formers, it has been an unalterable rule that interstitial apatite plaque is a white, flat suburothelial deposit of linear to plate like shape. By contrast, because they are constrained within tubules collecting duct apatite plugs are yellow, elongate, sausage-shaped, and sometimes nodular; their boundaries are regular and delimited, in contrast to the wandering map-like serpiginous shapes of interstitial plaque. When apatite plugs extend out of the mouths of ducts of Bellini, their appearances are particularly distinctive, in that they greatly dilate the openings of these ducts giving the papillary tip a "pitted" appearance. The number of pits is determined by how many collecting

ducts are plugged with apatite, and by how much the mass of deposit has enlarged the size of the lumen. Given the invariant relationships between appearance and histology we have found, clinicians can accurately assess the tissue basis for crystal deposits seen at surgery.

### Etiology is presently speculative

The fact that all brushite stone formers have interstitial apatite plaque like that found in calcium oxalate stone formers, and have an additional tubule lesion suggests brushite and calcium oxalate stone formers share a common pathogenesis. In fact, some of our brushite stone formers began with calcium oxalate stones. Urine calcium levels are generally high in these ten patients (Table 2), as they are in calcium oxalate stone formers, reflecting the well-known idiopathic hypercalciuria syndrome [4]. We propose that the interstitial plaque arises from the same combination of factors (high urine calcium, reduced urine volume, and reduced urine pH) we have documented as correlates of apatite plaque among calcium oxalate stone formers [3]. For reasons not as yet defined, the brushite patients deposit apatite in terminal collecting ducts, engendering the pathology of brushite stone disease.

Multiple factors may promote brushite stone formation. One case (Table 1, case 7) who was a uric acid stone former, was treated with large amounts of potassium alkali, and thereafter formed brushite stones. Another case (Table 1, case 4) had ureteropelvic obstruction as a child, with subsequent stones at age 7. Possibly chronic obstruction caused mild collecting duct cell injury [20].

Some of our patients had many ESWL procedures (Table 1). ESWL damages collecting duct cells [21], and renal papillary damage is always present after clinically relevant dosage of shock waves [22] in experimental animals. Such damage could reduce the ability of collecting ducts to regulate tubule fluid pH [23], so that luminal pH rises and fosters calcium phosphate crystallization [3]. Our present study cannot test the hypothesis that ESWL causes brushite stone formation. However, our detailed analysis of cortical injury does not support the hypothesis that ESWL is sufficient to account for the greater glomerular and interstitial disease of brushite stone formers. In particular, brushite stone formers have more cortical pathology allowing for ESWL. Age bore no relationship to cortical pathology. Even so, there was a general trend among all patients considered together for greater cortical atrophy/fibrosis as number of ESWL procedures increased. These results suggest a need for further studies of this particular issue.

## CONCLUSION

Our work delineates a hitherto undescribed kidney lesion in stone forming patients. Patients with brushite stones have interstitial apatite plaque, collecting duct plugging with apatite, patchy but often severe papillary interstitial fibrosis, and cortical pathology reflecting nephron loss, and are thereby distinguished from the common calcium oxalate stone formers and from the intestinal bypass stone formers. Being a more malignant lesion, brushite disease warrants aggressive efforts at stone prevention. In addition, clinicians may wish to notice that the type of stone formed can reflect renal pathology and analyze all stones; many of the present brushite stone formers initially formed calcium oxalate stones. Investigators may wish to note how essential stone type is for clinical phenotyping; had we mixed brushite and calcium oxalate stone formers, we would have missed an important point. Far from being a simple disorder within the urinary tract, stones involve renal crystallizations and tissue diseases we presently understand to only a very limited extent. Although brushite stone formers constitute perhaps 5% of all stone formers, millions of people have stones, so brushite-associated renal disease may not be rare. Recently, Vupputuri et al [24] have shown in a case-control study that history of kidney stones may be a risk factor for chronic kidney disease. Our findings here may therefore represent one pole of a broad spectrum of renal injuries related to stones in general. Finally, we call attention to the greater number of ESWL procedures in our brushite stone formers versus calcium oxalate stone formers, which may relate in part to the lesions we describe.

## ACKNOWLEDGMENT

This work was supported by NIH grants PO1 DK56788 and PO1 DK43881.

*Reprint requests to Andrew P. Evan, Department of Anatomy & Cell Biology, Indiana University School of Medicine, 635 Barnhill Drive, MS 5055, Indianapolis, IN 46220*
*E-mail: evan@anatomy.iupui.edu*

## REFERENCES

1. Stamatelou KK, Francis ME, Jones CA, *et al*: Time trends in reported prevalence of kidney stones in the United States: 1976–1994. *Kidney Int* 63:1817–1823, 2003
2. Evan AP, Lingeman JE, Coe FL, *et al*: Randall Plaque of patients with nephrolithiasis begins in basement membranes of thin loops of Henle. *J Clin Invest* 111:607–616, 2003
3. Parks JH, Worcester EM, Evan AP, *et al*: Clinical implications of abundant calcium phosphate in routinely analyzed kidney stones. *Kidney Int* 66:777–785, 2004
4. Werness PG, Brown CM, Smith LH, Finlayson B: Equil 2: A basic computer program for the calculation of urinary saturation. *J Urol* 134:1242–1244, 1985
5. Worcester EM: Stones due to bowel disease, in *Kidney Stones: Medical and Surgical Management*, edited by Coe F, Favus, M. Pak CYC, Parks J, Preminger G, Philadelphia, Lippincott-Raven, 1996, pp 883–903
6. Kuo RL, Lingeman JE, Evan AP, *et al*: Endoscopic renal papillary biopsies: A tissue retrieval technique for histologic studies in nephrolithiasis patients. *J Urol* 1170:2186–2189, 2003

7. Kuo R, Lingeman JE, Evan AP, *et al*: Urine calcium and volume predict coverage of renal papilla by Randall's plaque. *Kidney Int* 64:2150–2154, 2003
8. Yasue T: Histochemical identification of calcium oxalate. *Acta Histochem Cytochem* 2:83–95, 1969
9. Randall A: The etiology of primary renal calculus. *Intl Abst Surg* 71:209–240, 1940
10. Khan SR, Finlayson B, Hackett R: Renal papillary changes in patient with calcium oxalate lithiasis. *Urology* 23:194–199, 1984
11. Randall A: The origin and growth of renal calculi. *Ann Surg* 105:1009–1027, 1937
12. Low RK, Stoller ML, Schreiber CK: Metabolic and urinary risk factors associated with Randall's papillary plaques. *J Endourol* 14:507–510, 2000
13. Arsenault AL, Grynpas MD: Crystals in calcified epiphyseal cartilage and cortical bone of the rat. *Calcif Tissue Int* 43:219–25, 1988
14. Worcester EM, Parks JH, Thisted R, *et al*: Causes and consequences of kidney loss in patients with nephrolithiasis. *Kidney Int* 64:2204–2213, 2004
15. Jamison RL, Kriz W: Nephrons and collecting duct system, in *Urinary Concentrating Mechanism: Structure and Function*, Oxford University Press, New York, 1982, pp 35–43
16. Rao NR, Heptinstall RH: Experimental hydronephrosis. *Invest Urol* 6:183–204, 1968
17. Chevalier R: Pathophysiology of obstructive nephropathy in the newborn. *Semin Nephrol* 18:585–225, 1998
18. Kanwar YS, Mannaligod JR: Leukemic urate nephropathy. *Arch Pathol* 99:467–472, 1975
19. Simmonds HA, Sahota AS, Van Acker KJ: 1995 adenine phosphoribosyltransferase deficiency and 2,8-dihydroxyadenine lithiasis, in *The Metabolic and Molecular Bases of Inherited Disease*, edited by Scriver CR, Beaudet AL, Sly WS, Valle D, New York, McGraw-Hill, 1995, pp 1707–1724
20. Nagle RB, Bulger E, Cutler RE, *et al*: Unilateral obstructive nephropathy in the rabbit: Early morphologic, physiologic and histochemical changes. *Lab Invest* 28:456–467, 1973
21. Connors BA, Evan AP, Lingeman JE, *et al*: The effect of discharge voltage on renal injury and impairment caused by lithotripsy in the pig. *J Am Soc Nephrol* 11:310–318, 2000
22. Evan AP, Willis LR, Lingeman JE, McAteer JA: Renal trauma and the risk of long-term complications in shock wave lithotripsy. *Nephron* 78:1–8, 1998
23. Hamm LL, Alpern R: Cellular mechanisms of renal tubular acidification, in *The Kidney, Physiology and Pathophysiology*, edited by Seldin DW, Giebisch G, Philadelphia, Lippincott Williams & Wilkins, 1980, pp 1935–1980
24. Vupputuri S, Soucie JM, McClellan W, Sandler DP: History of kidney stones as a possible risk factor for chronic kidney disease. *Ann Epidemiol* 14:222–228, 2004